Journal of Intelligent and Robotic Systems **20:** 105–129, 1997.

Adaptive Impedance Control Applied to a Pneumatic Legged Robot

COSTAS S. TZAFESTAS, NACER K. M'SIRDI and N. MANAMANI
Laboratoire de Robotique de Paris (L.R.P.) 10-12 Av. de l'Europe, 78140 Velizy, France

(Received: 25 March 1997; accepted: 16 June 1997)

Abstract. An adaptive impedance control scheme with estimation of robot and environment parameters is proposed in this paper. It consists of two stages of adaptation and control. The first one performs an on-line estimation of the robot inertial parameters, during the complete (constrained or not) motion of the leg, while the second one compensates for the uncertainties on the characteristics of the ground (position and stiffness). Simulation results obtained for a single leg of a pneumatic driven, quadruped robot show the effectiveness of the proposed control scheme in case of considerable uncertainty both in the robot and ground parameters.

Key words: adaptive impedance control, passive feedback systems, robust control, pneumatic legged robot.

1. Introduction

Many robotics application tasks, like grasping and manipulating an object or assembling devices, inevitably involve direct interaction with the environment. Contact between the robot and the environment may also occur unpredictably due either to presence of unknown obstacles in the robot's workspace or to imprecision in positioning the robot end-effector. All the above situations may result in application of excessive and uncontrollable forces between the robot and its environment. The goal of a general force control methodology is to control these interaction forces in order to assure correct and safe execution of the robot task.

Whitney was the first one to report on the use of force feedback techniques in a computer-controlled manipulator [19]. Since then, various force control methodologies have been developed which can be classified in the following three major axes: impedance control, explicit force control and hybrid control.

Impedance control [5] is essentially a position control scheme where force feedback is used to modify the apparent inertia of the robot seen from the environment. The goal of this methodology is to explicitly regulate the compliance of the manipulator, i.e. its ability to yield under the application of external forces. These forces are then indirectly controlled by commanding the end-effector to follow an appropriate reference position trajectory. In explicit force control, on the contrary, the variable being directly measured and controlled is the external

force. The objective here is to follow a desired force trajectory defined in the task space (Cartesian coordinate system). The desired and measured force signals are compared and processed to provide an actuation signal directly to the process. Most existing work uses a subset of PID servo loop together with some form of linear or non-linear filtering [14, 20].

A methodology that tries to combine the advantages and the potential of a pure force and a pure position control scheme is the hybrid force/position control. Mason, in 1981, presented a formalization of this methodology in terms of defining the geometry of a compliant task and the appropriate control strategies. Craig and Raibert developed a hybrid control architecture where the partitioning of the Cartesian space in two, purely position or force controlled, subspaces is conveniently performed by a selection matrix [2]. Khatib has also proposed a hybrid force/position control architecture where the complete dynamic model of the robot, expressed in the task cartesian coordinate frame, is used [8].

All these control methodologies in general attempt to cope with the difficulties present in the execution of complex contact tasks, where motions and forces have to be taken into account simultaneously. The major problems encountered by such a methodology are:

- The problem of dynamic stability in case of unpredictable contact with a stiff environment.
- The problem of uncertainties in the dynamic parameters of the robot and compensation for its nonlinear characteristics.
- The uncertainty in the characteristics of the environment (stiffness, position).

In the last case, an insufficient control design can, in case of a contact with a stiff environment, lead to an under-damped or even unstable system. A robust or adaptive control methodology can be generally used to tackle this type of problem, but such a control scheme here should also take into account the forces of robot–environment interaction, before eventually proceeding in an on-line estimation of these dynamic characteristics.

We must also note that the use of force derivative or angular acceleration feedback in the control law must be avoided due to the noisy nature of signals supplied by force sensors and optical encoders.

The system considered in this paper is a single leg of a pneumatic-driven robot, called SAP, developed in our laboratory to study the dynamic problems related with walking machines (Figure 1). Dynamic interaction with an unknown environment is inherent in the complete motion of a walking mechanism. Our goal here is to design a force controller for a single leg in interaction with the ground, taking into account the above mentioned problems. To robustify the control system with respect to these external disturbances we develop an adaptive impedance control scheme consisting of two stages:

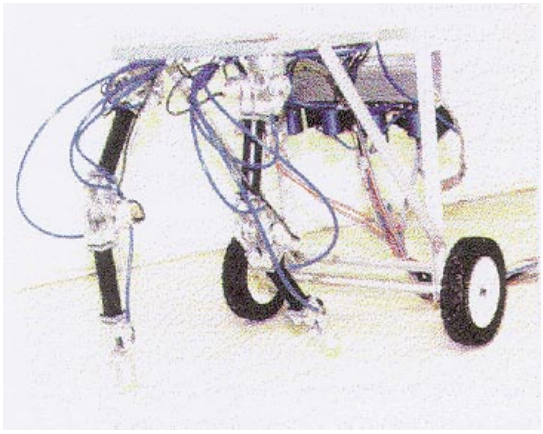

Figure 1. SAP pneumatic legged robot.

1. A first stage that compensates for the nonlinear characteristics and the uncertainty on the dynamic model of the leg, performing an on-line estimation of its dynamic parameters imposing the desired mechanical impedance. It constitutes the kernel of the control system and has to be active during the complete motion of the leg. This consists of a free motion phase (no contact with the ground, where the control objective is to closely follow a reference position trajectory), and a constrained motion phase, where we have to monitor and control the contact forces exerted on the endpoint of the leg.

2. A second stage of adaptation is necessary during the contact phase, in order to deal with the problem of uncertainty in the dynamic parameters of the ground and ensure the desired force trajectory tracking. As will be shown, one way of doing this is to perform an on-line estimation of the ground parameters (position and stiffness) during the contact phase, using the forces measured on the end-point of the leg.

This stage actually constitutes an external force compensation loop closed around the internal nonlinear impedance controller. A simple algorithm for the numerical computation of the defined impedance error is presented where only the available feedback information is used.

The paper is organized as follows. In Section 2 we present the dynamic model of the system used for the simulations. Section 3 starts by discussing the compensation of the pneumatic actuators dynamics and by presenting the overall control architecture of the system. A fixed impedance control law based on the computed torque control concept is presented in Section 3.3. The two stages of adaptation are therafter introduced (Sections 3.4 and 3.5) and stability analysis based on Lyapunov's theory is performed. Simulation results obtained for SAP's leg are presented in Section 4. Finally, Section 5 offers brief concluding remarks.

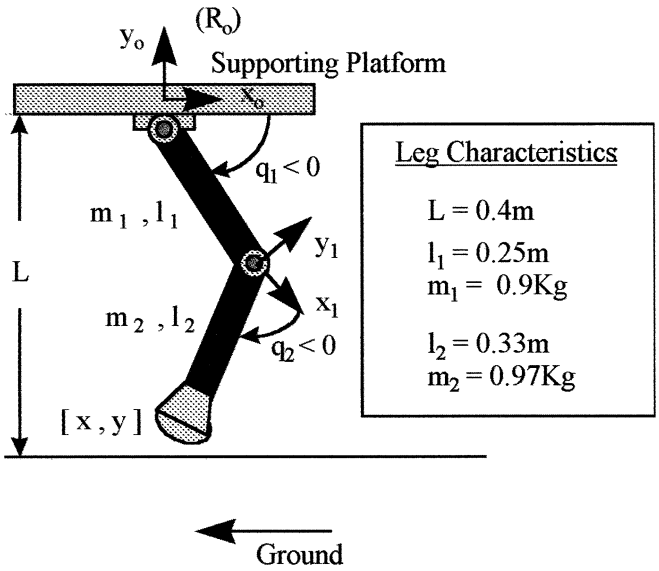

Figure 2. Kinematic model of the leg.

2. Modelling of the System

2.1. DYNAMIC MODEL OF A PNEUMATIC LEG

Each leg of the SAP robot has the kinematic structure of Figure 2. It consists of a supporting platform and two rigid links connected together with two rotational joints. The hardware configuration of the leg is presented by Figure 3. An incremental encoder is mounted on each joint to measure the angular displacements. In addition to that, a force sensor can be placed on the endpoint of the leg in order to measure the interaction forces with the ground. Each link is equipped with a pneumatic cylinder, an electropneumatic servovalve to control the pressure applied on the piston, and a piezoresistive sensor to measure the differential pressure z_i between the two chambers of each actuator. The linear motion of the piston is transformed in rotational motion through a cable.

The dynamic model of this rigid two link system can be written as:

$$M(q) \cdot \ddot{q} + h(q, \dot{q}) = \tau + J^T F_e, \tag{1}$$

where q denotes the 2×1 vector of joint angular positions ($q = [q_1, q_2]^T$), $M(q)$ is the 2×2 generalized inertia matrix of the robot, $h(q, \dot{q}) = C(q, \dot{q})\dot{q} + g(q)$ contains the Coriolis, centrifugal and gravitational terms, J is the Jacobian matrix of the robot, τ the actuator torques and F_e the external force applied on the endpoint of the leg.

For the torques τ applied by the pneumatic actuators on the leg joints we can obtain the following equation (see [13] for details):

$$\dot{\tau} + B \cdot \tau = G \cdot i - E \cdot \dot{q}, \tag{2}$$

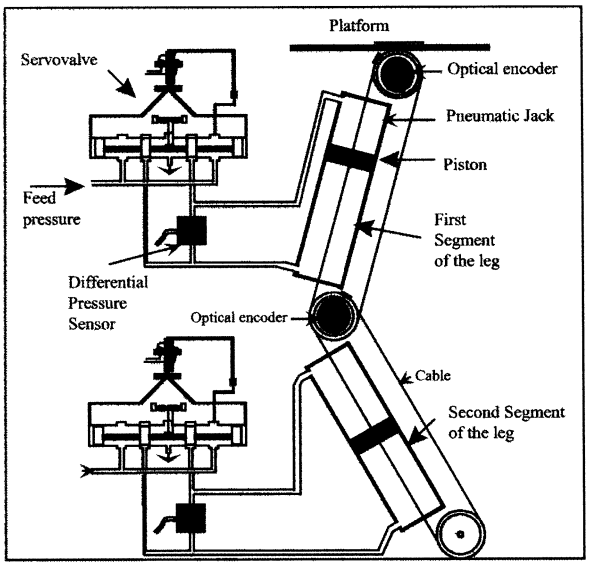

Figure 3. Hardware structure of the leg.

where B, G and E are 2×2 diagonal parameters matrices, depending on the actuators initial conditions, and i is a vector containing the input currents supplied in the servovalves. To obtain this equation some assumptions have been made, considering the displacement of the piston being due to small slide variations around its central position and the pneumatic system symmetric. If $z = [z_1, z_2]^T$ contains the differential pressures between the two chambers of each actuator $(z = P_p - P_n)$, we have:

$$\tau = k_0 \cdot S \cdot l \cdot z, \tag{3}$$

where S is the cross-section area of the piston and l the radius of the pulley. The differential pressures z_i are directly measured by the piezoresistive sensors.

2.2. ROBOT-ENVIRONMENT INTERACTION MODELLING

During the contact of the leg with the ground the compound systems leg + controller/force sensor/environment (ground) interact with each other by mutual application of forces. The models most oftenly used either to study the impact of a robot with its environment [6, 21] or to analyse its dynamic stability [1, 3], are the linear models of type inertia-damping-stiffness (see Figure 4). Let us suppose for simplicity that the stiffness K_f of the force sensor approaches infinity (compliance close to zero). In fact, this is equivalent in saying that K_e represents the effective stiffness of the whole {force-sensor/ground} and B_e the relevant damping coefficient. The whole {robot + controller} can be ideally represented

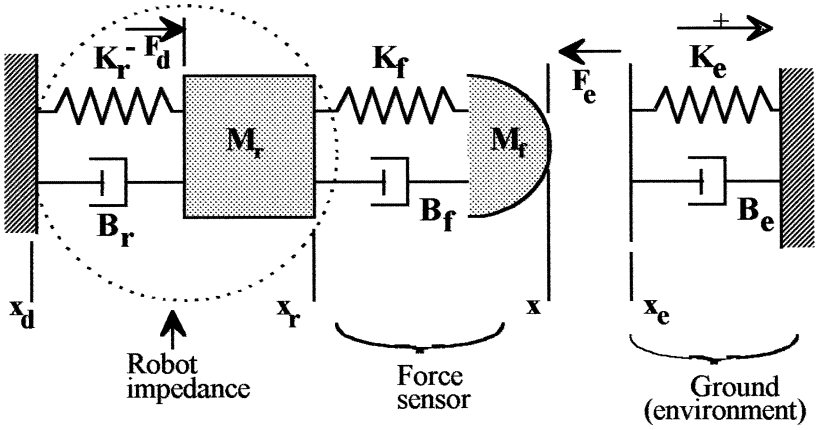

Figure 4. Robot-environment interaction model.

by the equivalent 2nd order impedance (M_r, B_r, K_r) imposed by the control law. We can then write the following equations:

$$F_e = K_e(x_e - x), \tag{4}$$

where x_e is the position of the ground, F_e the force applied on the end point of the robot leg, and

$$\left\{M_r p^2 + (B_r + B_e)p + (K_r + K_e)\right\} \cdot x = -F_d + K_r x_d + K_e x_e, \tag{5}$$

where x_d, F_d are the position and force reference signals, respectively, and x the end-point position of the robot. This system is linear, 2nd order and stable if $B_r, B_e > 0$. Its natural frequency is $\omega_n = \sqrt{(K_r + K_e)/M_r}$. If the ground is very stiff $(K_e \gg K_r)$, a choice of M_r less than a critical value may excite the neglected, high-frequency dynamics of the system, like flexibility of the links, delays in the control loop etc. This critical value, however, cannot be precisely known due to the uncertainty on the parameters of the ground. A trade-off must usually be found between free-motion speed and constrained-motion stability.

From Equations (4) and (5) in steady-state we obtain:

$$F_{ef} = F_e(t \to \infty) = \frac{K_e}{K_r + K_e} F_d + \frac{K_r K_e}{K_r + K_e}(x_e - x_d). \tag{6}$$

This equation will be used to study the force tracking capacity of the impedance controller during contact with the ground.

3. Two-stage Adaptive Impedance Control

3.1. COMPENSATION OF PNEUMATIC ACTUATORS DYNAMICS

The torque is controlled by a current i that is fed to the actuators' servovalves. Let us assume for simplicity of equations that G is known and $\widehat{B}$ and $\widehat{E}$ are

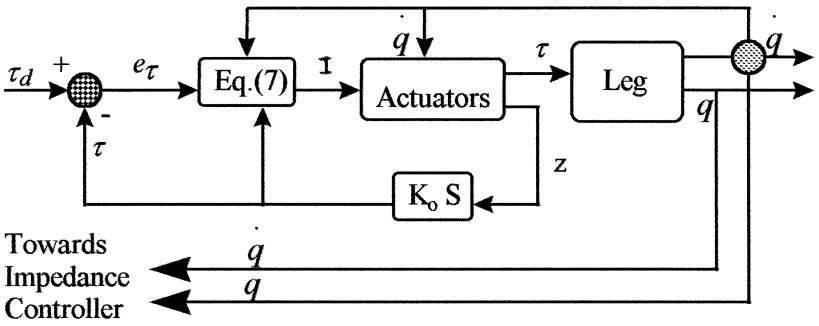

Figure 5. Compensation of actuators dynamics.

estimates of B and E respectively. In order to control the pneumatic actuators and compensate for their dynamic characteristics we can use an inner control loop of the form:

$$i = G^{-1} \cdot [u + \widehat{B} \cdot \tau + \widehat{E} \cdot \dot{q}] \quad \text{and} \quad u = K_\tau \cdot (\tau_d - \tau). \tag{7}$$

This is actually a feedback-linearization control law conceived from Equation (2) which describes the dynamic behaviour of the pneumatic actuators. We note also the presence of a current saturation at 20 mA. An adaptive version of control Equation (7) and an identification procedure for the pneumatic actuators characteristics have been recently developed in our laboratory [11, 13] (see Figure 5).

The objective of this control step is to allow us impose a desired torque to the leg joints using pneumatic actuators. Combining Equation (2) of the pneumatic leg with Equation (7) we obtain for the first (internal) control loop the following equation

$$\dot{\tau} + B \cdot \tau = K_\tau \cdot (\tau_d - \tau) + \widehat{B} \cdot \tau + \widehat{E} \cdot \dot{q} - E \cdot \dot{q},$$

$$K_\tau \cdot (\tau_d - \tau) = \dot{\tau} + \widetilde{B} \cdot \tau + \widetilde{E} \cdot \dot{q} \quad \text{with } \widetilde{B} = B - \widehat{B} \text{ and } \widetilde{E} = E - \widehat{E}.$$

This leads to $\tau = \tau_d - K_\tau^{-1}(\dot{\tau} + \widetilde{B} \cdot \tau + \widetilde{E} \cdot \dot{q}) \simeq \tau_d - 0(K_\tau^{-1})$.

This proves that with feedback pressure gain K_τ, we obtain an applied torque practically equal to the desired one. Physically, this is made possible by the fact that frequency characteristics of the electric part and pneumatic part (respectively about 200 Hz and 70 Hz for our case) of the system lead to faster dynamics with regard to the mechanical one. Implementing this internal control loop for pneumatic actuators allow us to focus our attention on the two steps of impedance control and adaptation regarding mechanical dynamics.

3.2. CONTROL ARCHITECTURE

The control architecture of the system is decomposed into two levels, as shown in Figure 6. The coordinator-level generates the position and force reference

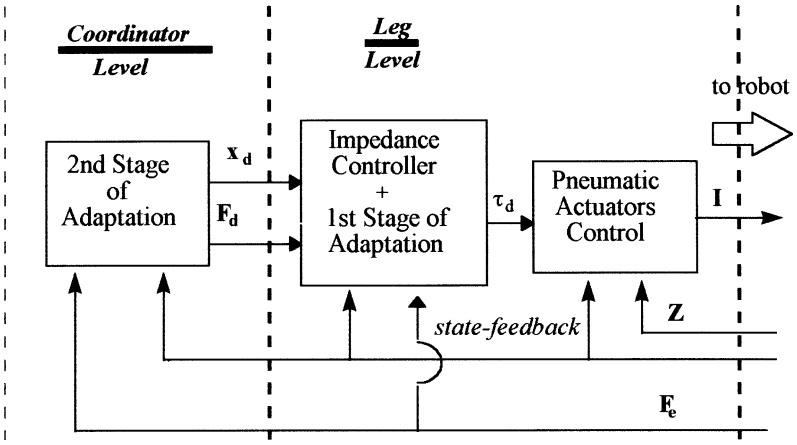

Figure 6. Control system architecture.

trajectories x_d and F_d respectively, which are afterwards supplied as command signals to the low-level control of each leg. The position reference trajectory can be chosen such as to ensure that the speed of the leg's endpoint at the moment of impact with the ground will be close to zero. We can also set a desired speed at this time instant by imposing a constant descent rate when approaching the ground. The ground is modelled as a conveyor belt with a constant horizontal speed of -0.1 m/s. In this control level we perform the second stage of adaptation, which is presented in Section 3.4. The goal of this adaptation stage is to ensure the desired force trajectory tracking during contact with the ground.

The leg-level performs the control of each joint and ensures the tracking of the position reference trajectory. In fact, the first control block has as its goal to impose the desired mechanical impedance on the leg, despite uncertainty in its dynamic parameters and interaction with the ground. The signal τ_d represents the desired control torque to be applied by the pneumatic actuators. An identification procedure for the pneumatic actuators characteristics has been recently developed in our laboratory, as discussed in the previous paragraph. In what follows, we focus our attention on the two stages of impedance control adaptation.

3.3. COMPUTED-TORQUE IMPEDANCE CONTROL LAW

The first step in implementing an impedance control scheme is to define the desired dynamic behaviour of the robot, that is the target-impedance. We choose a linear, second order model as the desired impedance:

$$M_r \cdot (\ddot{x}_d - \ddot{x}) + B_r \cdot (\dot{x}_d - \dot{x}) + K_r \cdot (x_d - x) = F_d - F_e \tag{8}$$

where x_d is the desired trajectory for the end point of the leg, F_d is the desired force reference trajectory and M_r, B_r, K_r are the desired apparent inertia, damping and stiffness matrix respectively.

The system dynamic equation is expressed in the cartesian coordinate frame R_0, fixed on the platform. This leads to the kinematic equation of the robot:

$$\dot{x} = J \cdot \dot{q} \Rightarrow \ddot{x} = J \cdot \ddot{q} + \dot{J} \cdot \dot{q} \tag{9}$$

as well as the static equation

$$\tau = J^T \cdot F. \tag{10}$$

The dynamic model of the robot rewritten in the same coordinate frame has the following form:

$$M^* \cdot \ddot{x} + h^* = F + F_e, \tag{11}$$

where M^* is the generalized inertia matrix expressed in the cartesian coordinate frame. We have:

$$M^* = Q^{-1}, \qquad Q = (J \cdot M^{-1} J^T) \tag{12}$$

and

$$h^* = J^{-T} \cdot h - M^* \cdot \dot{J} \cdot \dot{q}. \tag{13}$$

Assuming a perfect knowledge of the dynamic parameters of the robot, a linearizing control law for the implementation of the target impedance can be written as follows:

$$\tau = (J^T M^*) \cdot (u - \dot{J} \cdot \dot{q}) + h - J^T \cdot F_e. \tag{14}$$

The variable u is an auxiliary control signal which is chosen such that the closed-loop behaviour of the system is identical to the target impedance defined by Equation (8). From Equations (11) and (14) we obtain the closed-loop equation:

$$u = \ddot{x}. \tag{15}$$

In order to ensure that the closed-loop behaviour of the system is identical to the target impedance, the auxiliary control signal u must be chosen equal to:

$$u = \ddot{x}_d + M_r^{-1} \cdot \Big[K_r \cdot (x_d - G(q)) + B_r \cdot (\dot{x}_d - J(q) \cdot \dot{q}) - (F_d - F_e)\Big], \tag{16}$$

where $x = G(q)$ is the direct geometric model of the robot. The characteristics M_r, B_r, K_r of the target impedance are chosen so as to achieve the following goals:

- Ensure a satisfactory trajectory tracking in case of free motion of the leg. For this reason, matrices M_r, B_r, K_r can be chosen diagonal $M_r = \text{diag}[M_x, M_y]$, $K_r = \text{diag}[K_x, K_y]$ with values K_x/M_x and K_y/M_y sufficiently large to give the robot a fast trajectory tracking capability. B_x, B_y must provide a well damped behaviour.

- Ensure the stability of the whole system in case of contact with a stiff ground. For this reason M_x, M_y must be chosen greater than some minimum critical values, in order not to excite the unmodelled high frequency modes of the robot. In fact, M_r determines the force feedback gain matrix K_F, used implicitly in the control law (16). This gain matrix has the form:

$$K_F = (M^* \cdot M_r^{-1} - I_2), \tag{17}$$

where M^* is the effective inertia of the robot, M_r is the desired inertia and I_2 is the 2×2 identity matrix. It is, therefore, the external force feedback that allows us to modify the apparent inertia of the robot and impose the desired inertia term in the target impedance equation.

3.4. FIRST-STAGE: ON-LINE ESTIMATION OF THE LEG'S PARAMETERS

For the impedance control law presented in the previous paragraph we have assumed a perfect knowledge of the parameters in the dynamic model of the leg. In practice, however, the real values of these parameters cannot be precisely known in advance. This imprecision in the dynamic model of the robot has to be compensated for by the control law in order to robustify its dynamic behaviour. In what follows, an adaptive impedance control law is proposed which accounts for this uncertainty problem and a stability analysis based on Lyapunov theory is performed.

The control law (14) decribed in the previous paragraph is now replaced by the relation:

$$\tau = (J^T \widehat{M^*}) \cdot (u - \dot{J} \cdot \dot{q}) + \hat{h} - J^T \cdot F_e, \tag{18}$$

where $\widehat{M^*}$ and $\hat{h}$ denote the estimates of M^* and h respectively, and their values are adjusted on-line by an adaptation law. The goal here becomes that of designing such an adaptation algorithm in order to assure the stability of the whole system despite the existence of the modelling uncertainty. One can easily show that dynamic Equation (11) is linear on a set of robot parameters θ. If we consider the inertial parameters as the main source of uncertainty in the dynamic model of the robot, control equation (18) can be then written in the form:

$$\tau = J^T \cdot [\Phi^*(q, \dot{q}, u)\hat{\theta} - F_e] + \tau_c, \tag{19}$$

where $\tau_c = [\gamma_{1p}, \gamma_{2p}]^T$, the constant part of the torque.
Φ^* is the so-called regression matrix, with the difference that here it is computed for the cartesian model of the robot. It is a 2×4 known, nonlinear matrix, that depends on the geometry and the instantaneous configuration of the robot. $\hat{\theta}$ is a vector that contains the estimates for the inertial parameters of the robot, computed on line by the adaptation algorithm. If θ contains the real values of the robot parameters, we can equally write:

$$\begin{aligned}\Phi^*(q,\dot{q},u)\cdot\theta &= M^*\cdot u + h^* - J^T\tau_c \\ &= (J^{-T}MJ^{-1})\cdot[u-\dot{J}\cdot\dot{q}] + J^{-T}(h-\tau_c).\end{aligned} \tag{20}$$

3.4.1. *Stability Analysis*

Let $\tilde{\theta}=\theta-\hat{\theta}$ be the estimation error for the parameters of the robot. Combining Equations (11), (19) and (20) we have:

$$\Phi^*\cdot\tilde{\theta} = M^*\cdot(u-\ddot{x}). \tag{21}$$

We now define $\xi(e_d,e_F)$ an error signal:

$$\xi(e_d,e_F) = u-\ddot{x} = \ddot{e}_d + M_r^{-1}[B_r\cdot\dot{e}_d + K_r\cdot e_d - e_F]. \tag{22}$$

Equation (21) can then be rewritten in the form:

$$\Phi^*\cdot\tilde{\theta} = M^*\cdot\xi(e_d,e_F). \tag{23}$$

This is the cartesian-space error-dynamics equation, i.e. the dynamic behaviour of the system (position and force tracking error) with respect to the estimation error (disturbance in the model).

The error signal $\xi(e_d,e_F)$ can be interpreted as the so-called impedance error, that is an error with respect to the target-impedance dynamic model. In fact, in an impedance control methodology we are no longer interested in the position or force tracking error alone but in their dynamic relation as defined by the target-impedance equation. The goal here is to ensure that the closed-loop dynamic behaviour of the system follows as close as possible the model defined by the target-impedance equation (desired apparent inertia, damping and stiffness). This is equivalent with the convergence of the impedance error, as defined by Equation (22), to zero.

Let us define now a function $s=s(e_d,e_F)$ of the error such that:

$$\dot{s}+A\cdot s = \xi, \tag{24}$$

where A is a positive definite matrix. Integrating this equation we obtain:

$$s(t) = s(0) - \int_0^t As(t)\,\mathrm{d}t + \dot{e}_d + M_r^{-1}\left\{B_re_d + \int_0^t K_re_d\,\mathrm{d}t - \int_0^t e_F\,\mathrm{d}t\right\} \tag{25}$$

that gives the value of $s(t)$ directly from the available sensors information.

A similar methodology has been presented by [7, 12] who have introduced an impedance error in the following manner: $\xi = e_d - (F_e/Z_r)$, where Z_r is the target-impedance imposed on the robot. This definition leads to a different formalization for the error-dynamics of the system. The main difficulty of this approach in practice is the presence of the force derivative in the algorithm for

the computation of s, used trereafter in the adaptation law. This problem is here solved by Equation (25) where we make use only of the position e_d, velocity $\dot{e}_d$ and force e_F feedback (i.e., only the available feedback information).

In Appendix A we present two simple algorithms for the numeric computation of this signal s (also called "sliding surface" by [16] or error $\dot{e}_r$ with respect to the velocity reference model by [9]).

Let us now define as a Lyapunov-candidate function $V(t)$:

$$V(t) = \tfrac{1}{2} \cdot \left\{ \tilde{\theta}^T \Gamma \tilde{\theta} + s^T M^* s \right\}. \tag{26}$$

$V(t)$ is a non-negative energy function whose derivative is given by the equation:

$$\dot{V}(t) = \hat{\theta}^T \Gamma \tilde{\theta} + s^T M^* \dot{s} + \tfrac{1}{2} s^T \dot{M}^* s. \tag{27}$$

Combining Equations (27), (24) and (23) and defining the following relation:

$$\dot{\hat{\theta}} = \Gamma^{-1} \cdot (\Phi^*)^T \cdot s \tag{28}$$

we obtain

$$\dot{V}(t) = -(s^T (M^* A) s) \leqslant 0 \tag{29}$$

(M^*: positive definite and $A = \text{diag}(a_1, a_2)$ with $a_1, a_2 > 0$ which yields, for 2×2 matrices, $M^* A > 0$).

We therefore deduce that the system, with the defined relation (28), is asymptotically stable. In steady-state we have: $\dot{V} = 0 \Leftrightarrow s \equiv 0$ which means that $\xi(e_d, e_F) = 0$. The convergence of the impedance error to zero means that the imposed impedance on the leg, using the adaptive control law, approaches asymptoticaly the desired dynamic behaviour defined by the target-impedance equation.

Equation (28) defines the adaptation law which gives us, at each sampling period, the necessary modifications of the robot parameters estimates:

$$\hat{\theta}_{k+1} = \hat{\theta}_k + \Gamma^{-1} \Phi_k^{*T} \cdot s(k). \tag{30}$$

It constitutes, in fact, an Integral Parameter Adaptation Algorithm (P.A.A.) [9]. Simulation results for this control law, implemented on a single leg model of robot SAP, are presented in Section 4.

3.5. SECOND-STAGE: ADAPTATION IN FACE OF AN UNKNOWN ENVIRONMENT

3.5.1. *Uncertainty on the Parameters of the Ground and Force-Trajectory Tracking*

The key idea of the proposed method is to make an on-line estimation of the ground parameters K_e and y_e and then compute the desired end-point position trajectory, using these estimates.

As we have seen in Section 2.2, the force applied from the ground on the end point of the leg, in steady-state, is given by the equation:

$$F_{ef} = F_e(t \to \infty) = \frac{K_e}{K_r + K_e}(F_d + K_r(x_e - x_d)). \tag{31}$$

In order, therefore, to ensure the desired force trajectory tracking ($F_{ef} = F_d$) during contact with the ground, we should have:

– either

$$x_d = x_e - \left(\frac{F_d}{K_e}\right), \tag{32}$$

i.e., feed the appropriate position command to the impedance controller,

– or $K_r = 0$, i.e., modify the desired stiffness imposed by the impedance controller.

In fact, $K_r = 0$ means that the position error is no more taken into account, so that the control law actually becomes a pure force control law. However, in order to ensure the transition from a pure position control (free motion phase, no external forces) to a pure force control scheme (constrained motion phase, contact with the ground) we have to perform a switch in the parameters of the impedance control law. K_r has to change from a rather large value (position control) to a value equal or close to zero (force control). This discontinuity in the parameters of the control, as many researchers have reported, may cause instability problems in case of an unpredictable contact with a stiff environment. To avoid this situation, we have chosen the first approach, that is to command the desired position according to Equation (32), maintaining the kernel of the control system (first-stage adaptive impedance controller) intact, with no modification between the two different phases of motion. The control structure on its whole has been presented in Section 3.1 (Figure 6).

The position reference signal $X_d = [x_d, y_d]^T$ is therefore the one that is going to be modified during contact with the ground to assure a good trajectory tracking. These reference signals, during the contact phase, are computed from the following equations:

$$x_d(t) = \left(\frac{\Delta x}{\Delta t}\right) \cdot (-t + t_k) + x_{d0}, \tag{33}$$

$$y_d(t) = y_{d0}, \tag{34}$$

where Δx is the length of each step, Δt the duration of the contact phase, t_k the time instant of impact with the ground and x_{d0}, y_{d0} reference positions related with the ground parameters. If we knew in advance the exact position y_e of the ground and the value of its stiffness K_e precisely, we could calculate off-line the reference positions x_{d0} and y_{d0} to obtain the desired force F_d between the leg and the ground. y_{d0} could be calculated from the equation:

$$y_{d0} = y_e - \frac{F_d}{K_e}. \tag{35}$$

However, in practice the values y_e and K_e are not perfectly known and consequently we cannot obtain the desired force by simply using Equations (33)–(35). In what follows we use a method for the on-line adaptation of y_{d0} in order to ensure the force trajectory tracking without precise knowledge of the ground parameters (position and stiffness). This method is presented in [15]. Here it is integrated, as the second stage of adaptation, in the coordinator-level of the leg's impedance control structure.

3.5.2. *On-line Estimation of the Ground Parameters and Adaptation of the Position Reference Signals*

The key idea of this method is to make an on-line estimation of the ground parameters K_e and y_e and then compute the desired end-point position trajectory, using these estimates. From Equation (35) we can define y_{d0} as:

$$y_{d0} = \hat{y}_e - \frac{1}{\widehat{K}_e} \cdot F_d, \tag{36}$$

where $\hat{y}_e$ and $\widehat{K}_e$ are the estimates of y_e and K_e respectively. Let:

$$\hat{\theta}_e = [\widehat{K}_e, \widehat{K}_y]^T$$

be a vector containing the ground parameters estimates, where

$$\widehat{K}_y = \widehat{K}_e \cdot \hat{y}_e.$$

The actual force applied on the ground by the end point of the leg is:

$$F_e = K_e(y_e - y) = K_e y_e - K_e y = K_y - K_e y. \tag{37}$$

We can therefore define a prediction $\widehat{F}_e$ of the measured force F_e as follows

$$\widehat{F}_e = \widehat{K}_e(\hat{y}_e - y) = \widehat{K}_y - \widehat{K}_e y. \tag{38}$$

From the above equation we obtain:

$$\widehat{F}_e - F_e = [-y \quad 1] \cdot \tilde{\theta}_e.$$

The goal is now to find an adaptation law for $\widehat{K}_e$ and $\widehat{K}_y$, based on the prediction error $(\widehat{F}_e - F_e)$, in order to make $\widehat{F}_e \overset{t\to\infty}{\longrightarrow} F_e$. Let

$$V_e = \tfrac{1}{2} \cdot \tilde{\theta}_e^T \Gamma_e \tilde{\theta}_e, \tag{39}$$

where Γ_e is a 2×2 positive definite matrix (we can for instance set $\Gamma_e = \text{diag}[\gamma_{e1}, \gamma_{e2}]$, with $\gamma_{e1}, \gamma_{e2} > 0$).

We consider the Lyapunov function candidate:

$$V_{\text{cl}} = V + V_e = \tfrac{1}{2}\{s^T M^* s + \tilde{\theta}^T \Gamma \tilde{\theta}\} + \tfrac{1}{2}\tilde{\theta}_e^T \Gamma_e \tilde{\theta}_e. \tag{40}$$

Differentiating this equation (θ_e is considered constant) we obtain:

$$\dot{V}_{\text{cl}} = -s^T \cdot (M^* A) \cdot s - \tilde{\theta}_e^T \cdot \Gamma_e \cdot \dot{\hat{\theta}}_e.$$

Therefore, by defining the adaptation law as follows:

$$\dot{\hat{\theta}}_e = -\Gamma_e^{-1} \begin{bmatrix} -y \\ 1 \end{bmatrix} (\widehat{F}_e - F_e) \tag{41}$$

we obtain:

$$\dot{V}_{\text{cl}} = -s^T \cdot (M^* A) \cdot s - (\widehat{F}_e - F_e)^2 \leqslant 0. \tag{42}$$

We hence deduce that the closed-loop adaptive control system (stage I and II) is asymptotically stable. The first stage makes sure that in steady-state we will have:

$$K_r \cdot (y_{d0} - y) = F_d - F_e. \tag{43}$$

The steady-state equation for the 2nd stage of adaptation ($\widehat{F}_e = F_e$) can be written as:

$$F_e = F_d + \widehat{K}_e \cdot (y_{d0} - y). \tag{44}$$

Combining Equations (43) and (44) we obtain for the steady-state equation of the closed-loop system:

$$\left(1 + \frac{\widehat{K}_e}{K_r}\right)(F_d - F_e) = 0 \overset{\widehat{K}_e > 0}{\Leftrightarrow} (F_e = F_d) \tag{45}$$

which was the objective of the adaptive control during the leg-ground contact phase.

The adaptation law (41) can also be written as:

$$\left\{ \begin{array}{l} \widehat{K}_e = \gamma_{e1} \cdot y \cdot (\widehat{F}_e - F_e) \\ \hat{y}_e = \dfrac{\widehat{F}_e - F_e}{\widehat{K}_e} \cdot (-\gamma_{e2} - \gamma_{e1} \cdot y \cdot \hat{y}_e) \end{array} \right\}. \tag{46}$$

This adaptive control scheme, defined by Equations (36), (38) and (46), constitutes the second stage of adaptation.

4. Simulation Results

4.1. FIXED CONTROL LAW AND EFFECT OF THE DIFFERENT UNCERTAINTY SOURCES

We first consider the control law described in Section 3.3 by Equations (14) and (16). In this control law we suppose a perfect knowledge of the robot and ground parameters. The target-impedance characteristics are chosen as: $M_x = M_y = 1$,

$B_x = B_y = 30$ and $K_x = K_y = 225$. The ground is supposed to be very stiff with $K_e = 2 \times 10^5$ (Nt/m), $B_e = 150$ (Nts/m) and $y_e = -0.5$ m. For the force sensor we set $M_f = 250$ g, $B_f = 400$ (Nts/m) and $K_f = 4 \times 10^4$ (Nt/m). The effective stiffness of the environments is therefore: $K_{ef} = (K_e K_f)/(K_e + K_f) = (1/3) \times 10^5$ (Nt/m).

Let us suppose at first that the dynamic parameters of the robot and the environment (force sensor and ground) are precisely known. The reference position commanded during the contact phase will then be: $y_{d0} = y_e - (F_{dy}/K_{ef})$. Simulation results, for the complete motion of the leg, revealed that, as expected, with a perfect knowledge of the system dynamic parameters we can precisely regulate and control the interaction forces and achieve the impedance control objectives.

We start considering now the different sources of uncertainty and monitor their influence in the dynamic behaviour of the system. The goal is to approach the real conditions and analyse the robustness of the fixed impedance control law with respect to the different error sources (imprecisions in the dynamic model of the leg and uncertainties on the ground and force sensor parameters).

We first consider that the parameters of the leg are known with a 20% error: $e_m = e_I = 20\%$. The parameters estimates used in the impedance control law are therefore: $\widehat{m}_i = m_i(1 + e_m)$ and $\hat{I}_i = I_i(1 + e_I)$ $(i = 1, 2)$. We also add an imprecision of 2 cm on the estimated position of the ground. The simulation results obtained, for the complete motion of the leg during the first 8 s, are shown in Figures 7 and 8.

The different phases of this motion are the following:

(a) $0 < t < 2$ s, the leg takes its initial configuration;
(b) $2 < t < 3$ s, free motion of the leg, where its end point follows the reference position trajectory, given by the equation:

$$x_d = x_{d0} + r \cdot \Big[\omega \cdot (t - t_k) - \sin(\omega(t - t_k))\Big],$$

$$y_d = y_{d0} + r \cdot \Big[1 - \cos(\omega(t - t_k))\Big],$$

where t_k is the time instant for the beginning of each step;
(c) $3 < t < 4$ s, contact phase with the ground.

Along the x-axis the leg follows the relative movement of the ground while along the y-axis the leg is constrained by the ground.

The force reference signals are chosen as:

$$F_{dy} = F_{dy0} + C \cdot \left[\cos\left(\frac{\pi f t}{\beta}\right) - q \cdot \cos\left(\frac{3\pi f t}{\beta}\right)\right]$$

and

$$F_{dx} = v \cdot t \cdot F_{dy},$$

where C quantifies the fraction of the weight supported by each leg and v represents the mean horizontal speed of the leg's endpoint. β and q are parameters taken equal to $\beta = 0.75$ and $q = 0.2$.

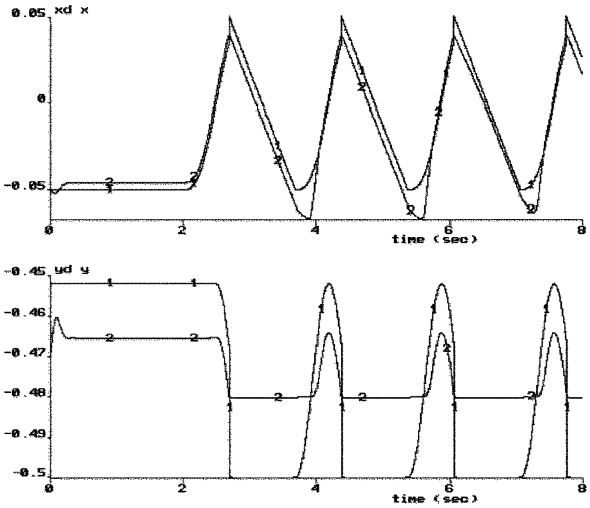

Figure 7. Motion of the leg's end point $[x, y]$ and reference position trajectory $[x_d, y_d]$ (fixed control law – no adaptation).

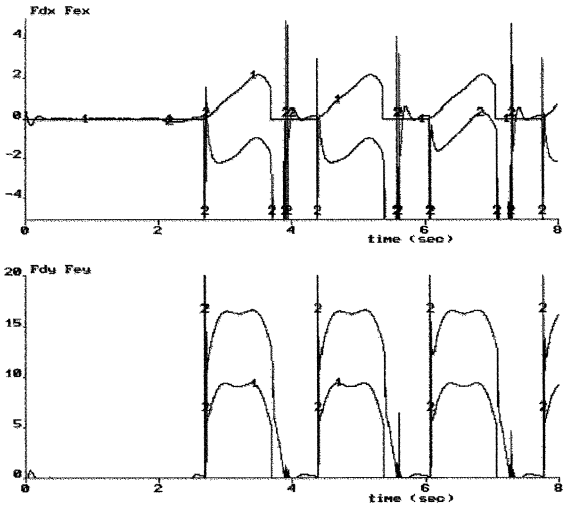

Figure 8. Force tracking (fixed control law).

The control objectives, thus, are: position trajectory tracking during free-motion of the leg (phase (b)) and desired force tracking during contact with the ground (phase (c)). These phase of motion repeat themselves periodically as shown by Figure 7. Figure 8 shows the force applied on the endpoint of the leg for the same period of time. Figure 9 shows the slipping of the endpoint of the leg during contact with the ground (slip $= 1$ when slipping of the leg occurs). We see clearly that the uncertainties introduced in the system result in slipping

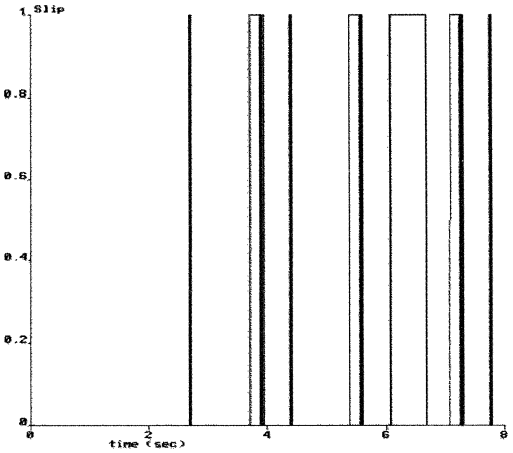

Figure 9. Slipping of the leg's endpoint on the ground.

of the leg during large periods of time, which may jeopardise the safe execution of the walking task.

Each source of uncertainty has its own effect in the degradation of the system's performance. The error in the dynamic parameters of the leg results in the existence of a steady state positioning error as well as a small force tracking error. The uncertainty on the parameters of the ground adds on the top of this a new component for the steady state force error deteriorating even more the force tracking characteristics of the system. In the following section we see how the two-stage adaptive impedance control, proposed in this paper, deals with this problem, compensating for the uncertainty in the dynamic parameters of the system as a whole.

4.2. TWO-STAGE ADAPTIVE IMPEDANCE CONTROL

Let us consider again that the parameters of the leg are not precisely known and that the vertical position of the ground, with respect to the supporting platform, is $y_e = -0.48$ m instead of -0.5 m (estimation error, 2 cm). We start by implementing the first stage of adaptation, described in Section 3.1. Let $\widehat{m}_1(t = 0) = \widehat{m}_2(t = 0) = 0.5$ kg and $\hat{I}_1(t = 0) = \hat{I}_2(t = 0) = 0$ be the initial estimates for the leg parameters. The simulation results obtained, for the same motion of the leg, are shown in Figures 10 and 11. The gains used in the adaptation law (30) are $\gamma_1 = \gamma_3 = \gamma_I = 0.001$, $\gamma_2 = \gamma_4 = \gamma_m = 2$ and $A = \text{diag}[a_j]$, $j = 1, 2$, $a_j = 15$.

From Figures 10 and 11 we derive the following conclusions:

The steady state position tracking error is now eliminated, thanks to the online estimation of the leg parameters. This adaptation stage thus robustifies the

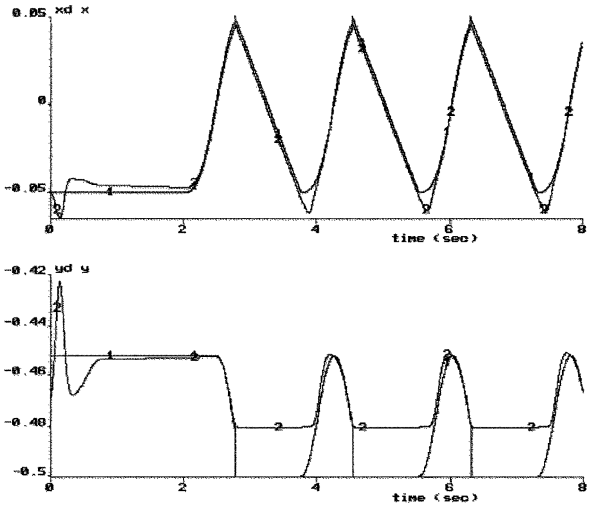

Figure 10. Position trajectory tracking (first stage of adaptation).

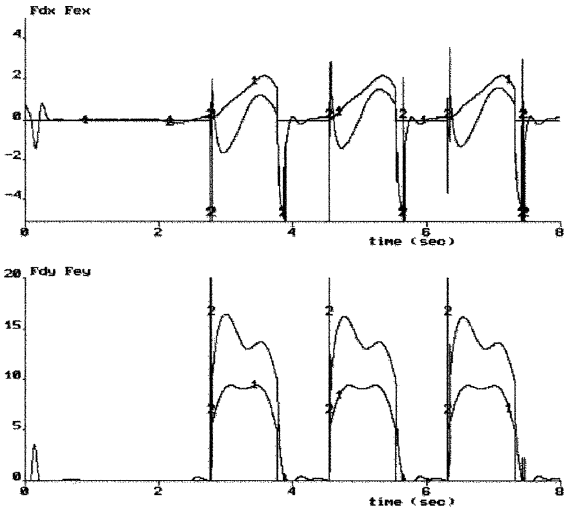

Figure 11. Force tracking (first stage of adaptation).

system with respect to imprecisions or unpredictable changes on the dynamic model of the leg for the complete, free-space or constrained, motion.

The force tracking error however persists, due to the uncertainty on the position and stiffness parameters of the ground and force sensor. Figure 12 shows the slipping characteristics of the system in this case. We may notice a clear improvement with respect to the results of the previous paragraph, when no adaptation was performed. However, important slipping of the leg during contact with ground still exists, which should be also due to the imprecision in the

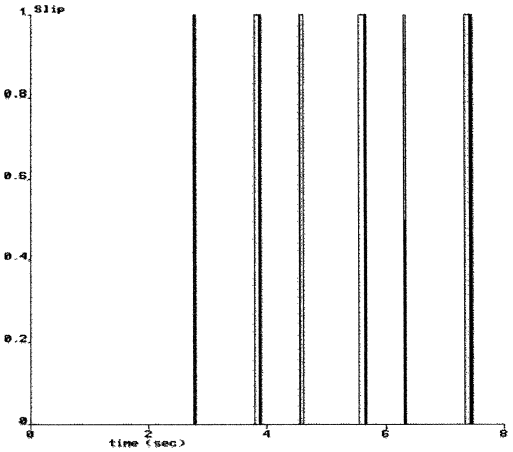

Figure 12. Slipping with first stage of adaptation (stage II not active).

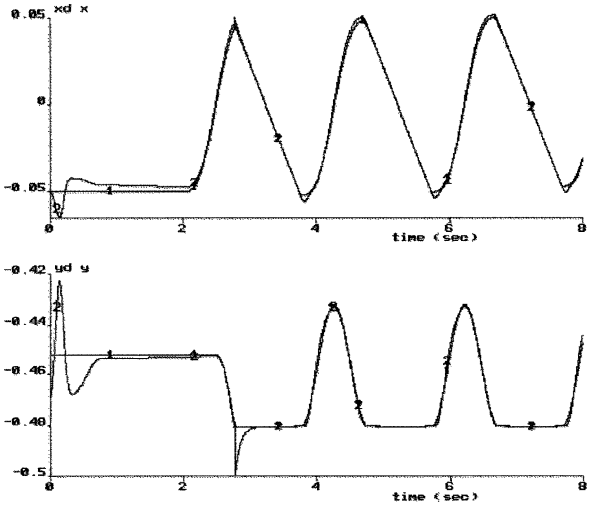

Figure 13. Position trajectory tracking (stage I and II active).

knowledge of the ground characteristics, and the insufficient programming of the position reference trajectories.

For this reason we now apply the second stage of adaptation as described by Section 3.5. The simulation results in this case are shown in Figures 13–18. The gains used for the second stage of adaptation are: $\gamma_{e1} = \gamma_{e2} = 10$ (see Equation (46)). We can clearly see that the force tracking error is now almost eliminated and that the transient response of the system is satisfactory. Notice the large force F_{ey}, and the important force error during the first contact with the ground which is afterwards eliminated, clearly demonstrating the action of the second stage of adaptation. The large values for F_{ex} and the light slipping at the

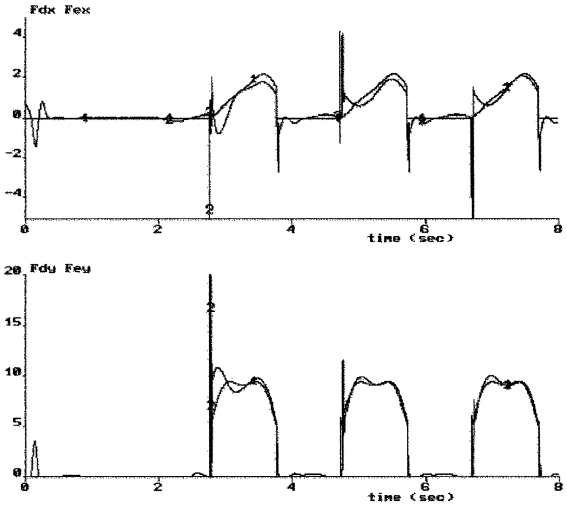

Figure 14. Force tracking (stage I and II active).

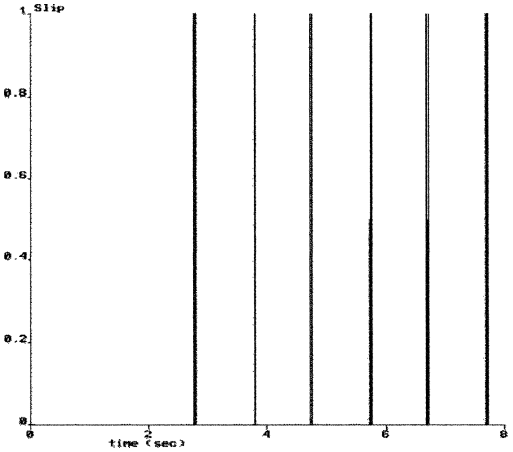

Figure 15. Slipping characteristics (stage I and II active).

time instants of contacting or leaving the ground are due to the discontinuities for the x_d reference signals at these time instants.

Figure 16 shows the actuators currents and torques during the complete motion of the leg. We notice the fact that saturation for the current (20 mA) is limited only on the first impact with ground, that is just before the second stage of adaptation starts acting.

Figures 17 and 18 shows the adaptation procedure for the robot m_i, I_i and ground K_e, y_e parameters respectively. We can observe that the estimates of these parameters converge towards some values which are approximately equal to the real ones. Moreover, the position (free motion) and force (constrained motion)

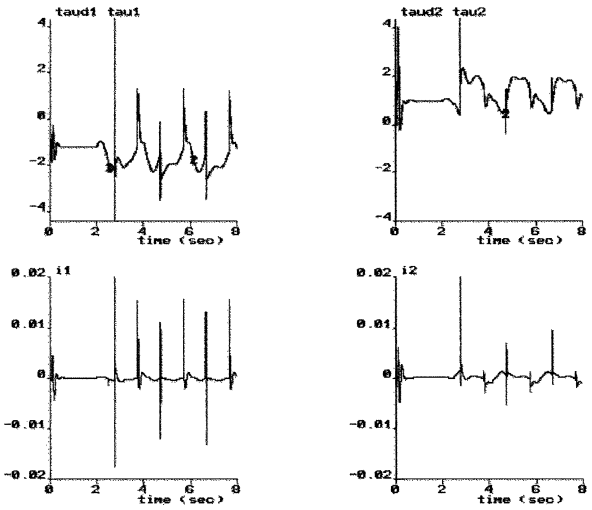

Figure 16. Actuators torques and currents.

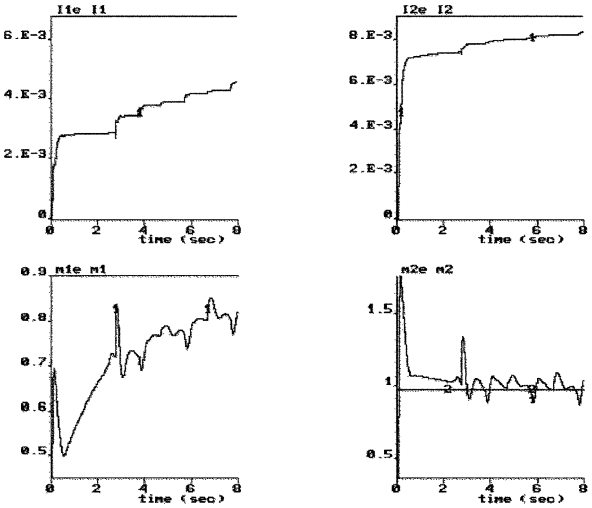

Figure 17. Robot parameters estimation (1st stage of adaptation).

tracking error converge rapidly to zero which was the objective of the whole control system during the two phases of motion.

5. Conclusion

A two-stage adaptive impedance control was proposed and applied for a single leg of a pneumatic driven robot. Our objective was to ensure the robustness of the system despite the presence of considerable uncertainties both in the robot and ground parameters. The first stage linearizes the dynamic behaviour

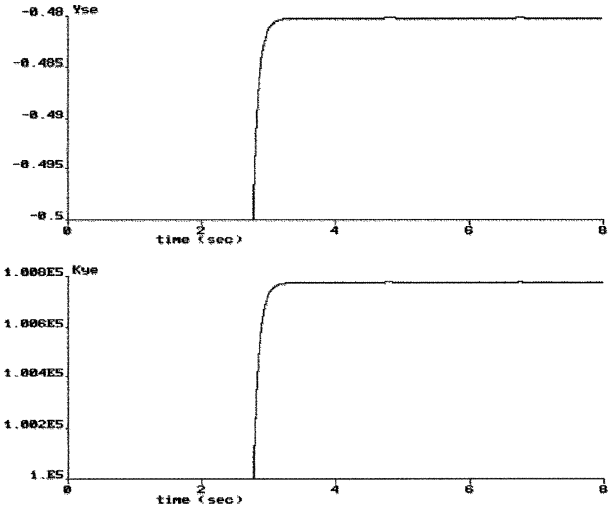

Figure 18. Ground parameters estimation (2nd stage of adaptation).

of the robot imposing the desired mechanical impedance, defined in terms of an apparent inertia, damping and stiffness matrix. It is based on a computed torque impedance control law where the robot parameters are estimated on-line using an integral parameter adaptation algorithm. The error signal used to update the robot parameters estimates is simply computed from the available feedback information. Measurements of joint acceleration as well as force derivative are not needed. The second stage performs an on-line estimation of the ground parameters (stiffness and location) adapting afterwards the position reference signals to ensure the desired force tracking during contact with an unknown environment. It constitutes in fact an external force control loop closed around the first stage adaptive impedance controller. Simulation results obtained for a pneumatic driven leg show the effectiveness of the proposed control scheme in case of considerable uncertainty both in the robot and ground parameters.

Appendix A

The numerical computation of the error signal $s(e_d, e_F)$ can be performed, using Equation (25), as follows:

$$s(k) = [\dot{e}_d + (M^{-1}B) \cdot e_d] + \text{integr}(k), \tag{A1}$$

$$\text{integr}(k+1) = \text{integr}(k) - A \cdot s(k) \cdot h + M^{-1}[Ke_d(k) - e_F(k)] \cdot h, \tag{A2}$$

where k is a given sampling instant and h the sampling period which has been taken equal to 3 ms.

This algorithm uses only the position, velocity and force feedback (i.e. the available in practice feedback information). Measurements of joint acceleration

or force derivative is therefore not needed for the computation of s. Numerical integration can also be performed using the trapezoidal rule as follows:

$$\begin{aligned}\text{integr}(k+1) \;=\; &\text{integr}(k) - A\cdot[s(k)+s(k-1)]\cdot\frac{h}{2}+\\ &+(M^{-1}K)[e_d(k)+e_d(k-1)]\cdot\frac{h}{2}-\\ &-(M^{-1})[e_F(k)+e_F(k-1)]\cdot\frac{h}{2}. \qquad \text{(A3)}\end{aligned}$$

Equation (A1) and (A2) or (A3) involve only a few simple arithmetic operations and are, therefore, easily implemented on a digital impedance control system.

References

1. An, C. and Hollerbach, J.: Dynamic stability issues in force control of manipulators, in: *Proc. of the 1987 IEEE Internat. Conf. on Robotics and Automat.*, 1987, pp. 890–896.
2. Craig, J. J. and Raibert, M. H.: A systematic method of hybrid position-force control of a manipulator, *J. Dynamic Systems Meas. Control* **103**(2) (1981), 126–133.
3. Eppinger, S. and Seering, W.: On dynamic models of robot force control, in: *Proc. of the 1986 IEEE Conf. on Robotics and Automat.*, pp. 29–34.
4. Guihard, M., Fontaine, J. G., and M'Sirdi, N. K.: Comparative study of adaptive controllers for a pneumatic driven leg, *IEEE/RSJ Internat. Conf. on Intelligent Robots and Systems* (IROS 1994).
5. Hogan, N.: Impedance control: An approach to manipulation, part I – Theory, part II – Implementation, part III – Applications, *J. Dynamic Systems Meas. Control* **107** (March 1985), 1–24.
6. Kahgn, J. and Amirouche, F. M.: Impact force analysis in mechanical hand design, in: *Proc. of the 1987 IEEE Conf. on Robotics and Automat*.
7. Kelly, R., Carelli, R., Amestegui, M., and Ortega, R.: Adaptive impedance control of robot manipulators, *International J. Robotics and Automation* **4**(3) (1989).
8. Khatib, O.: A unified approach for motion and force control of robot manipulators: The operational space formulation, *IEEE J. Robotics and Automat.* **RA-3**(1) (1987), 43–53.
9. Landau, I. D. and Horowitz, R.: Synthesis of adaptive controllers for robot manipulators using a passive feedback systems approach, in: *Proc. IEEE Conf. on Robotics and Automat.*, Philadelphia, USA, April 1988.
10. Mason, M. T.: Compliance and force control for computer controlled manipulators, *IEEE Trans. Systems Man Cybernet.* **SMC 11**(6) (1981), 418–432.
11. M'Sirdi, N. K., Khalil, W., Manamani, N., and Nadjar-Gauthier, N.: Identification and sliding mode control for a pneumatic leggend robot, *Internal Report*, Lab. de Robotique de Paris, Univ. Paris VI, Submitted to the *Internat. J. of Robotics Research*.
12. M'Sirdi, N. K. and Benali, A.: Adaptive impedance control for compliant motion in passive environments, in: M. Cotsaftis and F. Vernadat (eds), *Advances in Factories of the Future, CIM and Robotics*, Elsevier, 1993.
13. M'Sirdi, N. K., Manamani, N., and Gauthier, N.: Modeling and identification of a pneumatic legged robot, in: *IEEE-SMC IMACS*, Vol. IV, July 1996, pp. 803–880.
14. Qian, H. P. and De Schutter, J.: Introducing active linear and nonlinear damping to enable stable high gain force control in case of stiff contact, in: *Proc. IEEE Conf. on Robotics and Automat.*, pp. 1374–1379.
15. Seraji, H. and Colbaugh, R.: Adaptive force-based impedance control, in: *Proc. of the 1993 IEEE/RSJ Internat. Conf. on Intelligent Robots and Systems*, Yokohama, Japan, July 26–30 (IROS 1993), pp. 1537–1544.

16. Slotine, J. J. and Li, W.: Adaptive strategies in constrained manipulation, in: *Proc. IEEE Conf. on Robotics and Automat.*, 1987.
17. Tzafestas, C., Guihard, M., and M'Sirdi, N. K.: Two-stage adaptive impedance control applied to a legged robot, in: *IEEE/RSJ Internat. Conf. on Intelligent Robots and Systems* (IROS'95).
18. Volpe, R. and Khosla, P.: An experimental evaluation and comparison of explicit force control strategies for robotic manipulator, in: *Proc. IEEE Conf. on Robotics and Automat.*, Nice, France, May 1992, pp. 1387–1393.
19. Whitney, D. E.: Force feedback control of manipulator fine motions, *J. Dynamic Systems Meas. Control* (June 1977), 91–97.
20. Xu, Y. and Paul, R.: On position compensation and force control stability of a robot with a compliant wrist, in: *IEEE Conf. on Robotics and Automat.*, 1988, pp. 1638–1642.
21. Youcef-Toumi, K. and Gutz, D.: Impact and force control, in: *IEEE Conf. on Robotics and Automat.*, 1989, pp. 410–416.